GEORGE FOX UNIVERSITY

Digital Commons @ George Fox University

Faculty Publications - School of Physical Therapy | School of Physical Therapy

2005

Rabbit Knee Joint Biomechanics: Motion Analysis and Modeling of Forces during Hopping

David L. Gushue

Jeff Houck
George Fox University, jhouck@georgefox.edu

Amy L. Lerner

Follow this and additional works at: http://digitalcommons.georgefox.edu/pt_fac

 Part of the Physical Therapy Commons

Recommended Citation

Previously published in Journal of Orthopedic Research 23(4):735-42, 2005. Posted with permission. http://www.ors.org/journal-of-orthopaedic-research/

This Article is brought to you for free and open access by the School of Physical Therapy at Digital Commons @ George Fox University. It has been accepted for inclusion in Faculty Publications - School of Physical Therapy by an authorized administrator of Digital Commons @ George Fox University. For more information, please contact arolfe@georgefox.edu.

Rabbit knee joint biomechanics: Motion analysis and modeling of forces during hopping

David L. Gushue [a], Jeff Houck [a,b], Amy L. Lerner [a,*]

[a] *Department of Biomedical Engineering, 215 Hopeman Hall, University of Rochester, River Campus Box 270168, Rochester, NY, USA*
[b] *Department of Physical Therapy, Ithaca College, Rochester, NY, USA*

Abstract

Although the rabbit hindlimb has been commonly used as an experimental animal model for studies of osteoarthritis, bone growth and fracture healing, the in vivo biomechanics of the rabbit knee joint have not been quantified. The purpose of this study was to investigate the kinematic and kinetic patterns during hopping of the adult rabbit, and to develop a model to estimate the joint contact force distribution between the tibial plateaus. Force platform data and three-dimensional motion analysis using infrared markers mounted on intracortical bone pins were combined to calculate the knee and ankle joint intersegmental forces and moments. A statically determinate model was developed to predict muscle, ligament and tibiofemoral joint contact forces during the stance phase of hopping. Variations in hindlimb kinematics permitted the identification of two landing patterns, that could be distinguished by variations in the magnitude of the external knee abduction moment. During hopping, the prevalence of an external abduction moment led to the prediction of higher joint contact forces passing through the lateral compartment as compared to the medial compartment of the knee joint. These results represent critical data on the in vivo biomechanics of the rabbit knee joint, which allow for comparisons to both other experimental animal models and the human knee, and may provide further insight into the relationships between mechanical loading, osteoarthritis, bone growth, and fracture healing.

Keywords: Rabbit; Knee; Biomechanics; Kinematics; Joint loading

Introduction

The rabbit hindlimb has been commonly used as an in vivo experimental animal model in various types of orthopaedic research. Studies of osteoarthritis include those of induced mechanical instability [3,6,12,16,19–23,25,29,34,35], those focusing on alterations of knee joint load distribution [18,27,39], and those of chemically-induced osteoarthritis [4,15,33]. In addition, the rabbit hindlimb has been used extensively in studies of the relationships between load transmission, bone growth [1,2,5] and fracture healing [9,24,26,28]. Despite of this extensive use, little is known with regard to the in vivo biomechanics of the normal rabbit knee joint. For example, models of damage to the ligaments or soft tissues, such as ACL-transection, or meniscectomy are believed to alter both the magnitude and distribution of knee joint forces, therefore playing a primary role in the initiation and progression of osteoarthritis [31]. However, the relative distribution of medial and lateral joint contact forces in the rabbit knee during hopping, which is likely to be critical in the development of osteoarthritis, remains unknown.

In humans, dynamic gait parameters, such as the knee adduction moment, and the prediction of higher forces passing through the medial as compared to the lateral compartment of the knee, have been correlated with the presence of medial compartmental osteoarthritis [30,36]. Furthermore, a positive relationship has been

* Corresponding author. Tel.: +1 585 275 7847; fax: +1 585 276 1999.
E-mail address: amy.lerner@rochester.edu (A.L. Lerner).

identified between the predicted knee joint contact loads and bone density in the medial and lateral compartments of the proximal tibia in both healthy and osteoarthritic patients [10,36]. Although a strong predominance of medial compartmental loading has been well documented during human gait, the relative distribution of medial and lateral knee joint loading has never been quantified in the rabbit knee joint, even in studies reporting changes in biomechanics leading to osteoarthritis [18,39]. Mansour et al. [19] quantified the in vivo kinematics of the rabbit knee in an unstable model of osteoarthritis during the swing phase of hopping, however, the lack of both kinematic and kinetic data during the stance phase made predictions of tibiofemoral joint contact forces impossible.

Knowledge of the in vivo biomechanics of the normal rabbit knee joint will provide critical data for future experimental designs and may help explain findings in studies using the rabbit, and potentially other quadrupedal hindlimbs, as experimental models. Therefore, the purpose of this study was to investigate the normal hopping gait of the adult rabbit through calculations of three-dimensional intersegmental forces and moments, and to develop a model to estimate the medial and lateral joint contact forces on the tibial plateaus.

Material and methods

Knee kinematics and kinetics were determined in vivo in five skeletally mature male New Zealand White rabbits (Average weight = 3.6 kg). The University Committee on Animal Resources at the University of Rochester reviewed and approved all aspects of this study related to the care and treatment of the animals.

Surgical technique

To prevent soft tissue motion artifact associated with surface markers during the kinematic data collections, markers were attached to intra-cortical bone pins implanted into the tibia and femur of the rabbit. Following premedication of ketamine (IM 35 mg/kg) and xylazine (IM 5 mg/kg), lateral 1.0 cm incisions were made in the right femur and tibia under sterile conditions. Anesthesia was maintained using tracheal intubation and isoflurane gas (1–3%). Sterile Steinmann pins (threaded, stainless steel, 1.9 mm diameter, Howmedica Inc.) were introduced into the femur at the level of the third trochanter, and into the tibia at the level of the tibial tuberosity, using a cordless orthopaedic drill (Stryker Instruments). Beginning at the lateral cortex, both pins were driven until they pierced the medial cortex, and stainless steel nuts (low profile ~1.0 mm height) were threaded onto each pin and tightened down onto the surface of the bones with a sterile nut driver to prevent pin migration. After closure, antibiotic ointment (Iodophor PVP ointment, Aplicare Inc.) was applied to the pin-skin interface, and protective polypropylene balls (~19 mm diameter) were attached to the exposed heads of the pins to prevent the pins from becoming caught in the animal's cage.

Motion analysis

The rabbits were trained, both before and after surgery, to hop across two Kistler model 9286A force plates (Kistler Instrument Corp., Amherst, NY) mounted in the floor of a walkway, to measure the vertical (Fy), horizontal anterior posterior (Fx), and medial-lateral (Fz) ground reaction forces. Each force plate was connected to an 8-channel charge amplifier (Model 9865C, Kistler Instrument Corp., Amherst, NY) with the range set to 1000 [pC/10 V] for the X,Y, and Z-directions. A Plexiglas track was used to keep the animals moving straight ahead, with their ipsilateral pairs of limbs on separate force plates. During data collection, the protective polypropylene balls were removed, and three infrared emitting diodes (IREDs) were mounted on small acrylic disks attached to the implanted intra-cortical pins in both the tibia and femur. An additional set of three IREDs was placed on a holder strapped around the foot (Fig. 1). The IREDs were tracked in three-dimensional space using an Optotrak 3020 motion analysis system, with a manufacturer reported RMS accuracy of 0.1 mm (Northern Digital, Inc., Waterloo, Ontario, Canada). Kinematic and kinetic data were collected simultaneously with sampling rates of 60 Hz and 300 Hz, respectively. Prior to analysis, kinetic data were low-pass filtered at 15 Hz using a dual-pass Butterworth filter.

Anatomic coordinate systems for the foot, tibia, and femur were established by digitizing bony landmarks relative to the IRED coordinate system of each segment, with a pre-calibrated 6-marker digitizing probe. The tibial tuberosity, and both the medial and lateral malleoli were externally palpated, and their locations relative to the tibial IREDs were digitized and used to create an orthogonal coordinate system whose origin was located at the midpoint between the malleoli. Likewise, the third trochanter, and both the medial and lateral femoral epicondyles were externally palpated, and their locations relative to the femoral IREDs were digitized and used to create an orthogonal coordinate system whose origin was located at the midpoint between the femoral epicondyles.

Hopping trials recorded in which both a forelimb and, after a short interval, the ipsilateral hindlimb contacted the force plate were considered valid. To aid in the isolation of experimental data representing hindlimb contact (Fig. 2), each trial's kinetic data was coupled with simultaneous videotape obtained at 30 frames/second with a camera located at the level of the walkway, orthogonal to the direction of motion on the rabbit's right side. All trials selected for further analyses demonstrated a continuous hopping motion during which both hind feet contacted, and pushed off the force plates simultaneously. Furthermore, each trial was required to have a complete set of kinematic data

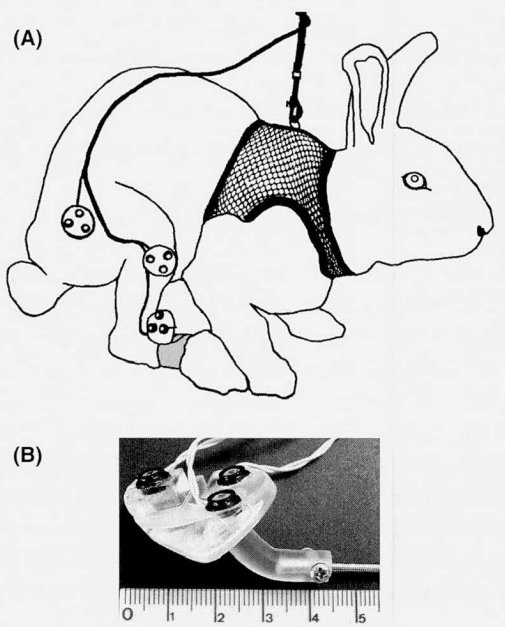

Fig. 1. Experimental setup for the kinematic data collections showing the location of the IREDs attached to the intra-cortical pins, including those used to track foot motion via an attached strap (A). Acrylic mounting device containing IREDs attached to intracortical pin (B). Note, the scale indicates centimeters.

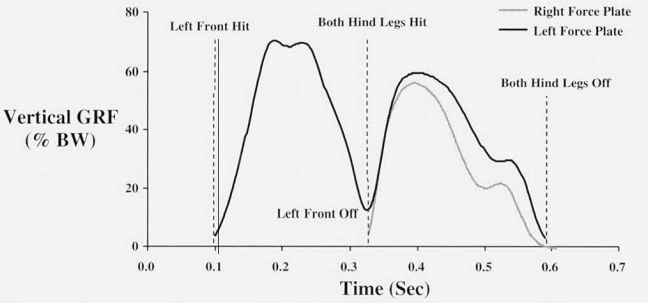

Fig. 2. The vertical ground reaction forces for a typical hopping trial consisted of two distinct paw strikes on each plate. Note, the rabbit's right front paw landed just beyond the edge of the force plate, therefore it is not measured during this trial.

with no marker dropout, as well as a clear identification of hindlimb contact on both force plates, thereby confirming the capture of kinetic data from only the limb of interest.

Modeling

The right hindlimb was modeled as a rigid link system, comprised of the femur, tibia and the foot. Based on preliminary studies that confirmed that the potential inertial effects due to linear and angular accelerations of the distal segments of the rabbit hindlimb during stance were negligible, the intersegmental forces and moments at both the ankle and knee were calculated throughout the stance phase of hopping by combining the ground reaction force data with anthropometric and position data using an inverse dynamic solution. The inverse dynamic analysis was calculated using a custom written FORTRAN computer program. Anthropometric data, including the center of mass locations and overall masses of the foot and shank segments, were measured using cadaveric hindlimbs from adult rabbits of the same age and weight as those used in this study. All kinematic and kinetic patterns were normalized to percent stance duration, from hindlimb foot strike to foot off, using a 1N threshold from vertical ground reaction force data.

A statically determinate model was used to predict muscle, ligament and tibiofemoral joint contact forces during the stance phase of hopping [8,10,30]. In addition to both medial (F_{MJC}) and lateral (F_{LJC}) tibiofemoral joint contact forces, the model included hamstrings (F_{Ham}), gastrocnemius (F_{Gast}), and patellar tendon (F_{Quad}) muscle forces, as well as medial (F_{MED}) and lateral (F_{LAT}) soft tissue forces, anterior (F_{ACL}), and posterior cruciate ligament (F_{PCL}) forces (Fig. 3). The hamstrings muscle group included the biceps femoris, semitendinosus and the semimembranosus, whereas the gastrocnemius muscle group included the medial and lateral heads.

Rabbit knee joint contact locations, muscle and ligament moment arms and lines of action were based on measurements obtained from magnetic resonance (MR) images (1.5 T clinical imaging unit, GE Medical Systems, Milwaukee WI). Using a phased array receiver coil, axial MR images of an intact cadaveric rabbit knee joint were acquired at a single flexion angle (Proton Density Sequence, TR = 2000, TE = 20, FOV = 6 cm × 6 cm, 0.9 mm Thickness, 0.3 mm Spacing, 256 × 192 Matrix). Area centroids and moment arms of each muscle and ligament cross-section were determined from multiple slices, and defined in a tibia anatomic coordinate system using a method similar to that previously reported for the identification of MR-derived human knee anatomic data [38]. Resultant force lines of action and moment arms for the included muscle groups were based on PCSA-weighted averages of the MR-based anatomic data for each individual muscle [17].

The muscle, ligament and joint contact forces were calculated by balancing their actions with the intersegmental forces and moments. As with other statically determinate mathematical models of the knee [8,10,30], the sagittal plane knee moment was balanced by activity of the flexor/extensor muscle groups. However, due to the biarticular nature of the gastrocnemius muscle group and the orientation of the intersegmental sagittal plane ankle moment (Fig. 4), it was possible to account for co-contraction of the gastrocnemius muscle group with the quadriceps. Hindlimb landing patterns during hopping created an external dorsiflexion moment at the ankle that was balanced by an internal plantarflexion moment (Fig. 4). Based on the PCSA of the gastrocnemius and plantaris muscles [17] that balance the ankle dorsiflexion moment, the contribution of the gastrocnemius muscle to balancing the intersegmental sagittal plane knee moment was calculated. The predicted gastrocnemius muscle forces were then transferred to the knee joint, where together with activity of the extensor muscle group, the intersegmental sagittal plane knee moment was balanced. The intersegmental anterior/posterior (A/P) forces were then balanced by the components of the calculated muscle forces in the AP directions and by forces in either the ACL or PCL, with the assumption that force in one cruciate implied that there was no force in the other [8,30]. The intersegmental frontal plane knee moment was then balanced by the components of the calculated muscle and cruciate ligament forces in the axial direction, the intersegmental axial knee force and the medial and lateral joint contact forces, which were each assumed to be represented by a single force, parallel to the tibial axis [8].

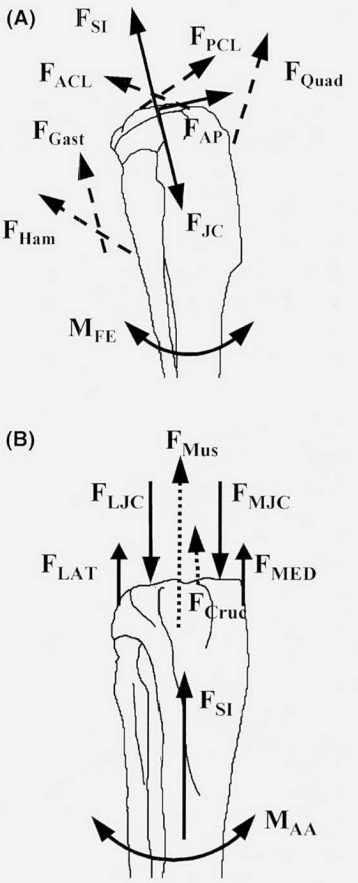

Fig. 3. Sagittal (A) and frontal (B) plane free body diagrams of the rabbit proximal tibia used in statically determinate model to calculate muscle and joint contact forces. Note, F_{Mus} represents the vertical component of the active muscle forces, as determined in the sagittal plane. Likewise, F_{Cruc} represents the vertical component of the active cruciate ligament.

Statistical analysis

To test for differences between animals, the peak values of each variable were analyzed with a single factor ANOVA. The peak values for each trial were then compared to determine if one or more typical gait patterns existed. After identification of two gait patterns, a two

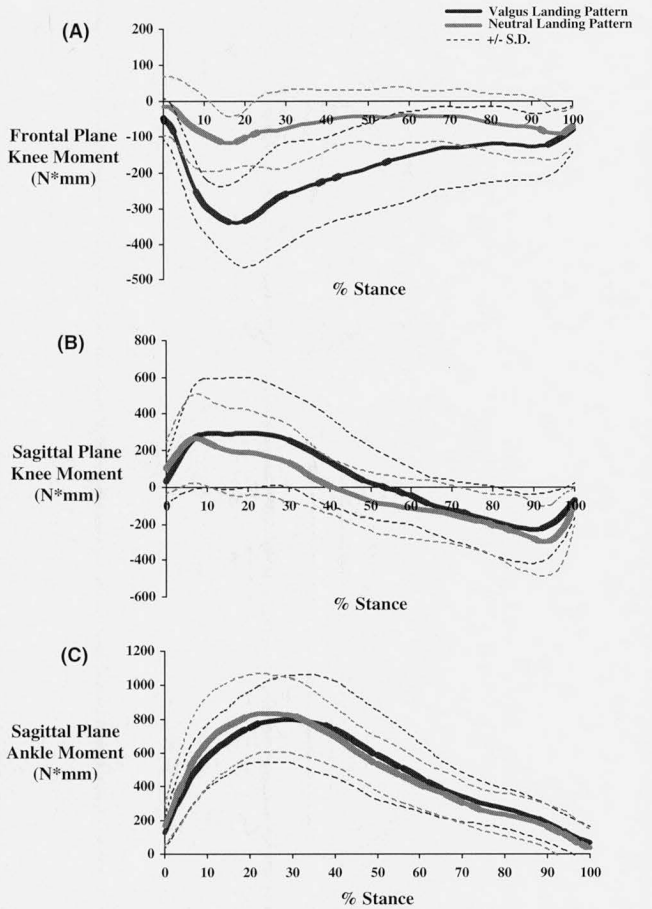

Fig. 4. The averages and standard deviations of the intersegmental frontal plane knee (A), sagittal plane knee (B), and sagittal plane ankle (C) moments for the two hindlimb landing patterns. All joint moments are expressed as positive values for external extensor, adductor and dorsiflexor moments.

factor (pattern and session) ANOVA was used to test for differences within each animal between data collection sessions. No significant differences were found between individual rabbits or data collection sessions, therefore all trials were pooled together for further analysis. To test for differences between patterns found, averages were calculated for each pattern in all rabbits and paired t-tests were used to determine the significance of differences between patterns for joint forces and moments, as well as predicted muscle and ligament forces. A p-value less than 0.05 was considered significant.

Results

The intra-cortical bone pin insertion surgery was well tolerated and all rabbits returned to normal weight-bearing within one week of the procedure, as determined by close observation and comparisons of both pre- and post-surgical force plate data. Each animal underwent multiple data collection sessions over a period of one- to two months, with an average of fifty data trials collected per session. However, the majority of the data trials were subsequently discarded due to either an inability to clearly identify hindlimb contact or more generally, a lack of a continuous hopping motion. In total, 41 successful data trials were collected, with each animal having a minimum of seven successful data trials spread over a minimum of three data sessions.

In all trials, forelimb vertical ground reaction force magnitudes were consistently higher than those of the hindlimb during hopping, and both hindlimbs were evenly and simultaneously loaded (Fig. 2). Likewise, all trials exhibited similar vertical ground reaction force patterns with two distinct paw strikes on each force plate, representing the ipsilateral fore- and hindlimbs, with the hindlimb strike exhibiting a characteristic two-peaked pattern.

Kinematic variability of the hindlimb position during landing created large variations in the intersegmental frontal plane knee moment. However, these differences could not be attributed to differences between animals or data collection sessions. Therefore, as shown in Fig. 4 and all subsequent figures, all data trials were categorized as either a valgus or neutral landing pattern, based upon differences in their frontal plane hindlimb kinetics: Pattern 1—Valgus landing pattern (19 data trials), Pattern 2—Neutral landing pattern (22 data trials). All animals displayed both landing patterns, with a minimum of three data trials for each landing pattern. By convention, in this paper we refer to external joint moments and all joint moments shown in Fig. 4 are expressed as positive values for extensor, adductor and dorsiflexor moments.

At initial hindlimb contact, the vertical ground reaction force passed lateral to the knee joint, which led to an increasing external knee abduction moment until approximately 15–20% of stance (Fig. 4(A)). A significant difference in the magnitude of the peak intersegmental knee abduction moment was found between the neutral and valgus hindlimb landing patterns ($p < 0.001$) (Table 1).

At initial hindlimb contact, the vertical ground reaction force passed anterior to both the knee and ankle joints, which led to increasing external knee extension and ankle dorsiflexion moments (Fig. 4(B) and (C)). As the rabbit proceeded through midstance, at approximately 40–55% of stance, the vertical ground reaction force passed through the knee joint, thereby creating no moment at the knee. During the latter portion of the stance phase, an external knee flexion moment and decreasing ankle dorsiflexion moment were present. No significant differences in the magnitude of the peak intersegmental knee flexion and extension moments (Table 1), or ankle dorsiflexion moments were found between the neutral and valgus landing patterns.

Upon hindlimb contact the intersegmental axial knee force increased sharply, reaching its peak of approximately 40% of body weight between 15% and 25% of stance (Fig. 5). As the rabbit proceeded through mid-

Table 1
External intersegmental forces and moments at the knee, and internal muscle, ligament, and tibiofemoral joint contact forces (mean ± std dev) of the peak values for both of the hindlimb landing patterns and the entire data set

	Valgus pattern (Mean (SD))	Neutral pattern (Mean (SD))	Overall (Mean (SD))
*Intersegmental forces (% BW) and Moments (N * mm)*			
Anterior force	2.4 (2.3)	1.5 (1.2)	1.9 (1.8)
Posterior force	3.6 (1.4)	3.8 (1.1)	3.7 (1.2)
Axial force	40.1 (9.9)	40.1 (9.5)	40.5 (9.6)
Abduction moment	391.4 (75.8)*	173.5 (68.8)	274.5 (131.0)
Flexion moment	271.5 (182.5)	351.2 (197.5)	314.3 (192.6)
Extension moment	403.0 (269.7)	320.5 (232.4)	358.7 (250.7)
Muscle and ligament forces (% BW)			
Quadriceps	310.9 (116.0)	290.2 (96.7)	299.8 (105.2)
Gastrocnemius	138.7 (43.4)	147.8 (37.4)	143.6 (40.0)
Anterior Cruciate Ligament	147.4 (58.0)	130.9 (48.7)	138.6 (53.2)
Tibiofemoral joint contact forces (% BW)			
Medial joint contact force	235.1 (108.7)	285.9 (94.1)	262.3 (103.2)
Lateral joint contact force	352.1 (86.9)*	262.2 (75.7)	303.8 (92.1)
Ratio of peak joint contact forces			
Medial force to lateral force	0.65 (0.22)*	1.11 (0.28)	0.89 (0.25)

Note: ACL peak forces may include contributions from other soft tissues restraining motion in the anterior direction.
* Indicates significant difference between valgus and neutral hindlimb landing patterns, $p < 0.05$.

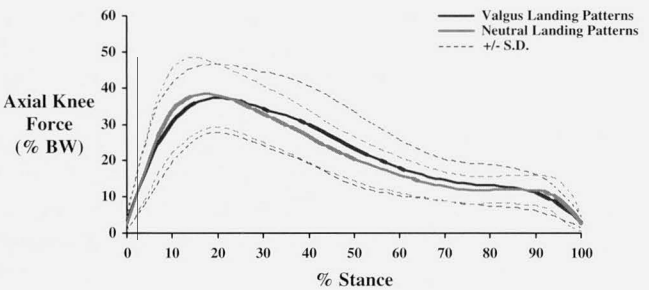

Fig. 5. The averages and standard deviations of the intersegmental axial knee forces for the two hindlimb landing patterns.

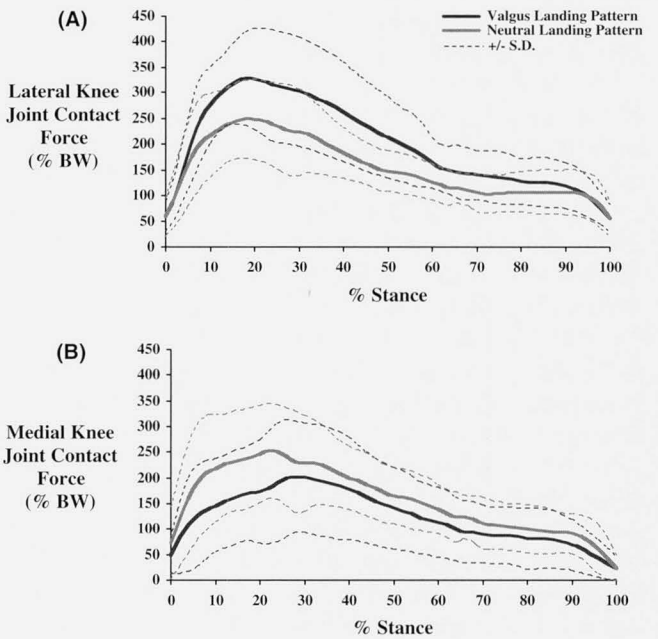

Fig. 6. The averages and standard deviations of the estimated lateral (A) and medial (B) tibiofemoral joint contact loads for the two hindlimb landing patterns.

stance toward toe-off, the intersegmental axial knee force gradually decreased. No significant difference in the magnitude of the peak intersegmental axial knee force was found between the neutral and valgus landing patterns (Table 1).

Our statically determinate mathematical model predicted significantly greater ($p < 0.001$) lateral tibiofemoral joint contact forces during the stance phase of the trials designated as a valgus landing pattern as compared to those of the neutral landing pattern (Fig. 6(A)). Furthermore, the valgus landing trials produced increased lateral tibiofemoral joint contact forces as compared to medial tibiofemoral joint contact forces (Fig. 6(B), Table 1). On average, the ratio of the peak joint contact force on the medial tibial plateau to that on the lateral plateau for the valgus landing pattern was 0.65 (Table 1). The neutral landing trials produced similar tibiofemoral joint contact forces on both the lateral and medial tibial plateaus during hopping, with an average ratio of the peak joint contact forces on the medial tibial plateau to that on the lateral tibial plateau of 1.11 (Table 1). This difference in the average ratio of the medial to lateral peak joint contact forces between the hindlimb landing patterns was found to be significant ($p < 0.001$). However, none of the predicted muscle and ligament forces, or the intersegmental anterior or posterior knee forces were significantly different between the two hindlimb landing patterns (Table 1).

Discussion

This study represents the first three-dimensional investigation of the kinematics and kinetics of the rabbit knee joint during normal activity, and therefore provides data that may be critical in the design and interpretation of studies of osteoarthritis, bone growth and fracture healing. As opposed to a static analysis of a single point in time, hindlimb kinematics and kinetics, including the distribution of tibiofemoral joint contact forces throughout the complete stance phase of normal hopping are presented. Although the force plate kinetics and hindlimb joint center locations collected during the motion analysis were similar for all trials, further modeling identified two distinct patterns of knee joint loading in the rabbit while hopping. More specifically, due to differences in frontal plane knee and ankle kinematics, the data exhibit large variations in intersegmental knee frontal plane moments, and subsequently the distribution of tibiofemoral joint contact forces. However, no significant differences were found in the sagittal plane kinematics or kinetics between the neutral and valgus landing patterns, thereby confirming the need for a complete three-dimensional analysis including both hindlimb kinematics and kinetics.

We have demonstrated the ability to calculate the in vivo distribution of tibiofemoral joint contact loads between the tibial plateaus during hopping with the development of a statically determinate mathematical model. In contrast to previously published models, which did not include antagonistic muscle forces [8, 10,30], our model utilized the combination of the biarticular nature of the gastrocnemius muscles and the predominance of an external dorsiflexion moment at the ankle, as a means for the inclusion of some degree of muscular co-contraction. This calculation of co-contraction results in increased muscle, and ultimately joint contact forces, thereby preventing the prediction of condylar liftoff often associated with previous statically determinate mathematical models [8,10,30]. The lack of ligamentous pre-tension, and the limited degree of co-contraction may still underpredict the actual joint contact forces in the knee, however the model provides a realistic estimate of the balance between the medial and lateral tibial plateaus.

Our modeling estimated an average peak patellar tendon force during level hopping of 105.8 ± 37.1 N. Juncosa et al. [11] reported an average in vivo peak patellar tendon force of 67.9 ± 0.9 N in adult New Zealand White rabbits during treadmill hopping, as measured with implantable force transducers. Although our predictions of peak patellar tendon forces during hopping are slightly higher, they might be explained by the fact that the rabbits in our study were not favoring their limb during the recorded activities (Fig. 2). Juncosa et al. [11] verified the balance of ground reaction forces during quiet sitting as a measure of hindlimb lameness, as opposed to those during dynamic hopping tasks. However, we found that the return to equal weightbearing during dynamic activities was slower than for the quiet sitting position.

In humans, dynamic gait parameters, such as the intersegmental knee adduction moment and the prediction of higher forces passing through the medial compartment of the knee joint have been correlated with the presence of osteoarthritis, as well as the distribution of proximal tibial bone density in normal and osteoarthritic subjects [10,30,36]. In addition, Hurwitz et al. [10] reported an average ratio of the peak joint contact forces on the medial tibial plateau to that on the lateral plateau of 2.2 ± 0.9 for healthy human subjects. In contrast, our study demonstrated the prevalence of an external intersegmental abduction moment during normal rabbit hopping, which was directly correlated with the prediction of higher forces passing through the lateral as compared to the medial compartment of the knee joint. We found an average ratio of the peak joint contact forces on the medial to that on the lateral tibial plateau of 0.65 ± 0.22 and 1.11 ± 0.28 for the valgus and neutral landing patterns respectively. In addition, the average ratio of the peak joint contact forces on the medial tibial plateau to that on the lateral plateau for all hopping trials, regardless of landing pattern was 0.89 ± 0.25. Therefore, despite the large variations in hindlimb landing patterns, and the subsequent magnitude of the intersegmental knee frontal plane moment, the prevalence of lateral compartment tibiofemoral joint loading during hopping is clear.

Previous studies that have used rabbit hindlimbs in experimental animal models have found an increased bone mineral density of the lateral tibial plateau as compared to the medial plateau [20], as well as a balanced distribution of subchondral tissue volume fraction between the medial and lateral tibial plateaus [37]. These experimental results are in agreement with the predictions of the in vivo biomechanics of the rabbit knee joint from our study, which clearly identified a prevalence of lateral compartment tibiofemoral joint loading during hopping. Therefore, caution should be used when comparing the results of an experimental study using the rabbit as an in vivo animal model, to those studies involving humans, as the normal biomechanics of the knee are very different.

Similar to rabbits, several canine studies [13,14,32] have identified either a balanced distribution, or a trend toward increasing modulus and bone volume fraction in the lateral compartment. Therefore, it may be instructive to compare the frontal plane kinetics in rabbits from our study, to those of other quadrupeds who walk rather than hop. These comparisons may enhance our current understanding of the influence of biomechanics on the development of osteoarthritis in experimental animal

models and would provide important information to aid in our understanding of the link between studies using animal models and both clinical and experimental observations in humans.

A limitation of this study that resulted in relatively small numbers of trials, was the inefficiency with which data was collected and subsequently discarded due to a lack of a continuous hopping motion; defined by a trial during which the animal's forward progression did not stop while on the force plate and a straight path of motion was maintained, as indicated by the video tape. However, we felt that it was important to capture the in vivo knee joint biomechanics during natural, uncontrolled movements, rather than using more constrained motion on a treadmill. Another limitation, which was subsequently resolved by tightening stainless steel nuts onto the surface of the bone during the pin insertion surgery, was pin loosening and associated rotation during the data collections. These rotations introduced small errors into our early report of rabbit knee joint intersegmental forces and moments [7]. However, comparisons of joint center estimates from quiet sitting trials taken both before and after the hopping data trials verified the absence of relative motion between the implanted pins and the associated bones during the data collections for this study. A final possible limitation in our study was the assumption that muscle and ligament moment arms and lines of action remain constant through varying knee flexion. To evaluate the sensitivity of our joint contact model predictions this potential variability, we performed a parametric analysis using previously published variations of these input parameters for the human knee [38]. We identified an average variation of less than 2% body weight for either the medial or lateral tibiofemoral joint contact forces, thereby minimizing the potential for these simplified model inputs to effect our model predictions.

In summary, our current study provides critical data on the normal in vivo biomechanics of the rabbit knee joint, which may provide further insight into the relationships between mechanical loading, osteoarthritis, bone growth, and fracture healing. Knowledge of the relative distribution of tibiofemoral joint contact loads represents critical data for the design and interpretation of both theoretical and experimental studies involving the rabbit hindlimb, other animal models, and potentially those involving the human knee.

Acknowledgements

This work was supported by funding from the Whitaker Foundation, and NSF-REU #EEC-0097470. The authors are grateful for surgical assistance provided by Dr. Faruk Abuzzahab as well as technical assistance provided by Emily Gedbaw and Jason Long.

References

[1] Alberty A, Peltonen J, Ritsilä V. Effects of distraction and compression on proliferation of growth plate chondrocytes: A study in rabbits. Acta Orthop Scand 1993;64:449–55.

[2] Alberty A, Peltonen J, Lindberg L-A. Early ultrastructural changes of the growth plate chondrocytes after compression and distraction of the physis in rabbits. Eur J Musculoskel Res 1993;2:18–24.

[3] Amiel D, Toyoguchi T, et al. Long-term effect of sodium hyaluronate (Hyalgan®) on osteoarthritis progression in a rabbit model. Osteoarthritis Cartilage 2003;11:636–43.

[4] Anastasiou A, Hall LD. A novel RF coil configuration for in-vivo and ex-vivo imaging of arthritic rabbit knee joints. Magn Reson Imaging 2003;21:61–8.

[5] Bonnel F, Peruchon E, et al. Effects of compression on growth plates in the rabbit. Acta Orthop Scand 1983;54:730–3.

[6] Colombo C, Butler M, et al. A new model of osteoarthritis in rabbits: Development of knee joint pathology following lateral meniscectomy and section of the fibular collateral and sesamoid ligaments. Arthritis Rheum 1983;26:875–86.

[7] Gushue DL, Long J, Houck J, Lerner AL. Motion analysis and mathematical modeling of the forces in the adult rabbit knee joint during hopping. Proc ASME Summer Bioeng Conf 2003:0893.

[8] Harrington IJ. Static and dynamic loading patterns in knee joints with deformities. J Bone Joint Surg Am 1983;65:247–59.

[9] Holmström T, Paavolainen P, Slätis P, Karaharju E. Effect of compression on fracture healing: plate fixation studied in rabbits. Acta Orthop Scand 1986;57:368–72.

[10] Hurwitz DE, Sumner DR, Andriacchi TP, Sugar DA. Dynamic knee loads during gait predict proximal tibial bone distribution. J Biomech 1998;31:423–30.

[11] Juncosa N, West JR, et al. In vivo forces used to develop design parameters for tissue engineered implants for rabbit patellar tendon repair. J Biomech 2003;36:483–8.

[12] Karakurum G, Karakok M, et al. Comparative effect of intra-articular administration of hyaluronan and/or cortisone with evaluation of malondialdehyde on degenerative osteoarthritis of the rabbit's knee. Tohoku J Exp Med 2003;199:127–34.

[13] Kuhn JL, Goldstein SA, Ciarelli MJ, Matthews LS. The limitations of canine trabecular bone as a model for human: a biomechanical study. J Biomech 1989;22:95–107.

[14] Kuhn JL, Goulet RW, Pappas M, Goldstein SA. Morphometric and anisotropic symmetries of the canine distal femur. J Orthop Res 1990;8:776–80.

[15] Laurent D, Wasvary J, O'Byrne E, Rudin M. In vivo qualitative assessments of articular cartilage in the rabbit knee with high-resolution MRI at 3 T. Magn Reson Med 2003;50:541–9.

[16] Le Graverand MP, Eggerer J, et al. Assessment of specific mRNA levels in cartilage regions in a lapine model of osteoarthritis. J Orthop Res 2002;20:535–44.

[17] Lieber RL, Blevins FT. Skeletal muscle architecture of the rabbit hindlimb: Functional implications of muscle design. J Morphol 1989;199:93–101.

[18] Lovasz G, Llinas A, et al. Effects of valgus tibial angulation on cartilage degeneration in the rabbit knee. J Orthop Res 1995;13:846–53.

[19] Mansour JM, Wentorf FA, Degoede KM. In vivo kinematics of the rabbit knee in unstable models of osteoarthrosis. Ann Biomed Eng 1998;26:353–60.

[20] Messner K, Fahlgren A, Ross I, Andersson B. Simultaneous changes in bone mineral density and articular cartilage in a rabbit meniscectomy model of knee osteoarthrosis. Osteoarthritis Cartilage 2000;8:197–206.

[21] Messner K, Fahlgren A, Persliden J, Andersson BM. Radiographic joint space narrowing and histologic changes in a rabbit

meniscectomy model of early knee osteoarthritis. Am J Sports Med 2001;29:151–60.
[22] Moskowitz RW, Davis W, et al. Experimentally induced degenerative joint lesions following partial meniscectomy in the rabbit. Arthritis Rheum 1973;16:397–405.
[23] Moskowitz RW, Goldberg VM. Studies of osteophyte pathogenesis in experimentally induced osteoarthritis. J Rheumatol 1987; 14:311–20.
[24] Murray DW, Wilson-MacDonald J, et al. Bone growth and remodeling after fracture. J Bone Joint Surg Br 1996;78:42–50.
[25] Pelletier JP, Fernandes JC, et al. In vivo selective inhibition of mitogen-activated protein kinase kinase 1/2 in rabbit experimental osteoarthritis is associated with a reduction in the development of structural changes. Arthritis Rheum 2003;48:1582–93.
[26] Prat J, Juan JA, et al. Load transmission through the callus site with external fixation systems: theoretical and experimental analysis. J Biomech 1994;27:469–78.
[27] Reimann I. Experimental osteoarthritis of the knee in rabbits induced by alteration of the load bearing. Acta Orthop Scand 1973;44:496–504.
[28] Richards M, Goulet JA, et al. Bone regeneration and fracture healing. Clin Orthop 1998;355S:S191–204.
[29] Sah RL, Yang AS, et al. Physical properties of rabbit articular cartilage after transection of the anterior cruciate ligament. J Orthop Res 1997;15:197–203.
[30] Schipplein OD, Andriacchi TP. Interaction between active and passive knee stabilizers during level walking. J Orthop Res 1991;9: 113–9.
[31] Setton LA, Elliott DM, Mow VC. Altered mechanics of cartilage with osteoarthritis: human osteoarthritis and an experimental animal model of joint degeneration. Osteoarthritis Cartilage 1999; 7:2–14.
[32] Sumner DR, Willke TL, Berzins A, Turner TM. Distribution of young's modulus in the cancellous bone of the proximal canine tibia. J Biomech 1994;27:1095–9.
[33] Vasilev V, Merker HJ, Vidinov N. Ultrastructural changes in the synovial membrane in experimentally-induced osteoarthritis of rabbit knee joint. Histol Histopathology 1992;7:119–27.
[34] Vignon E, Bejui J, et al. Histological cartilage changes in a rabbit model of osteoarthritis. J Rheumatol 1987;14(Supp 14):104–6.
[35] Wachsmuth L, Keiffer R, et al. In vivo contrast-enhanced micro MR-imaging of experimental osteoarthritis in the rabbit knee joint at 7.1T. Osteoarthritis Cartilage 2003;11:891–902.
[36] Wada M, Maezawa Y, et al. Relationships among bone mineral densities, static alignment and dynamic load in patients with medial compartment knee osteoarthritis. Rheumatology (Oxford) 2001;40:499–505.
[37] Wei X, Räsänen T, Messner K. Maturation-related compressive properties of rabbit knee articular cartilage and volume fraction of subchondral tissue. Osteoarthritis Cartilage 1998;6:400–9.
[38] Wretenberg P, Nemeth G, Lamontagne M, Lundin B. Passive knee muscle moment arms measured in vivo with MRI. Clin Biomech 1996;11:439–46.
[39] Wu DD, Burr DB, Boyd RD, Radin EL. Bone and cartilage changes following experimental varus or valgus tibial angulation. J Orthop Res 1990;8:572–85.